PNAS RESEARCH ARTICLE | AGRICULTURAL SCIENCES OPEN ACCESS

Soil organic nitrogen rather than fertilizer drives dinitrogen losses in flooded rice systems

Yuanyuan Lei[a,b,1], Zhijun Wei[a,b,1], Kaiye Ye[a,b], Kees Jan van Groenigen[c], Yu Liu[a,b], Hongna Cui[a,b], Klaus Butterbach-Bahl[d,e], Pete Smith[f], Deli Chen[g], Shu Kee Lam[g], William R. Horwath[h], Wulf Amelung[i,j], Chaopu Ti[a,b], Wei Zhou[a], Jingrui Yang[a,b], Hongbo He[k], Xudong Zhang[k], Sheng Zhou[l], Xiaoyuan Yan[a,b,2], and Longlong Xia[a,b,2]

Affiliations are included on p. 11.

Edited by Donald R. Ort, University of Illinois Urbana-Champaign, Urbana, IL; received February 3, 2026; accepted March 23, 2026

Rice production underpins food security but relies heavily on nitrogen (N) fertilization, much of which is lost as gaseous emissions. Dinitrogen (N_2) represents the largest N loss, yet its sources remain poorly constrained because biological dinitrogen (N_2) fluxes are difficult to quantify against the atmospheric background. Here, we apply an in situ ^{15}N tracing–membrane inlet mass spectrometry (^{15}N–MIMS) technique to simultaneously measure N_2, ammonia (NH_3), and nitrous oxide (N_2O) emissions and partition their soil- versus fertilizer-derived origins across the growing season in conventional *japonica* rice and hybrid rice. We find that soil organic N (SON) accounts for most N_2 emissions (72 to 75%), overturning the prevailing assumption that fertilizer dominates this loss pathway, which is independently confirmed by a 14-y fertilization experiment. In contrast, NH_3 originates mainly from fertilizer (71 to 77%) and N_2O derives from both sources in near-equal proportions. We identify a previously unrecognized "microbial N pump", in which rapid microbial assimilation of fertilizer-derived ammonium (NH_4^+) induces stoichiometric imbalance and stimulates SON mineralization, mobilizing soil-derived NH_4^+ that ultimately fuels N_2 emissions, with depleted SON partially replenished through microbial N turnover. Neglecting SON contributions causes systematic overestimation of fertilizer-derived N_2 and NH_3 losses by ~35%. Hybrid rice increases yield by 59% and reduces yield-scaled gaseous N losses by 43% through enhanced fertilizer uptake and microbial N use efficiency. Together, these findings reveal an underappreciated pathway of fertilization-driven soil N losses, revise N budgets for flooded rice systems, and demonstrate that cultivar-informed management can simultaneously enhance rice productivity and environmental sustainability.

nitrogen cycling | flooded rice field | gaseous nitrogen losses | dinitrogen measurement | ammonia volatilization

Significance

Flooded rice fields lose large amounts of nitrogen as dinitrogen (N_2), yet the sources of this loss remain unclear. Using a cutting-edge in situ isotopic technique, we show that most N_2 emissions arise not from fertilizer, as widely assumed, but from soil organic nitrogen mineralized by fertilization-stimulated microbial processes, termed as a microbial nitrogen pump. This hidden pathway highlights a previously overlooked source of soil-derived nitrogen loss, causing conventional methods to overestimate fertilizer-derived losses. Our findings revise nitrogen budgets for rice systems and highlight the need to manage soil–plant–microbe interaction to sustain rice yields while reducing N_2 losses. Hybrid rice cultivars markedly lower yield-scaled gaseous nitrogen losses by enhancing plant and microbial nitrogen use efficiency while maintaining high productivity.

Rice (*Oryza sativa*) is the main staple food for over half of the global population, providing more than 20% of global calorie intake (1). To meet rising demand, particularly in China—the world's largest producer and consumer of nitrogen (N) fertilizer (2, 3)—substantial amounts of N are applied to paddy fields. Application rates in China typically reach 200 to 300 kg N ha^{-1} per season, two to three times higher than in other major rice-producing countries such as Japan (80 to 100 kg N ha^{-1}) and India (100 to 150 kg N ha^{-1}) (3). However, rice plants often recover less than 40% of applied N, with about half lost to the environment (4, 5). Gaseous N emissions such as dinitrogen (N_2) and ammonia (NH_3) dominate these losses, accounting for up to ~50% of applied N, whereas hydrological losses through leaching and runoff contribute only 5 to 7% (6, 7). Quantifying and mitigating gaseous N losses are therefore critical for improving N use efficiency and ensuring sustainable rice production.

Nitrogen fertilizer has long been considered the main source of N_2 emissions from flooded paddy fields (8), where anaerobic conditions promote denitrification of fertilizer-derived nitrate or nitrite to N_2 via nitrous oxide (N_2O) intermediates (9, 10). However, N fertilization also stimulates microbial decomposition of soil organic matter (SOM), primarily in the oxygenated rhizosphere (11), as microbes decompose SOM to restore nutrient stoichiometric balance during the assimilation of fertilizer N. This process may function as a microbially driven pump, mobilizing soil organic N (SON) and releasing soil-derived ammonium (NH_4^+) that may contribute substantially to N_2 emissions. Direct quantification of soil- versus fertilizer-derived N_2 remains lacking, largely because measuring N_2 fluxes against a high atmospheric background is technically challenging. Previous estimates, based on methods like acetylene inhibition, ^{15}N tracing or mass balance—each with inherent limitations—suggest that N_2 emissions account for 22 to 41% of applied

The authors declare no competing interest.

This article is a PNAS Direct Submission.

[1]Y. Lei and Z.W. contributed equally to this work.

[2]To whom correspondence may be addressed. Email: yanxy@issas.ac.cn or llxia@issas.ac.cn.

This article contains supporting information online at https://www.pnas.org/lookup/suppl/doi:10.1073/pnas.2603983123/-/DCSupplemental.

Published April 22, 2026.

N fertilizer (6, 12, 13). Recent advances in membrane inlet mass spectrometry (MIMS) technique have enabled precise, direct measurement of N_2 fluxes in flooded systems (14, 15). Soil-core incubation studies using MIMS reported N_2 losses of 11.9 to 13.5% of applied fertilizer (16, 17), but these estimates may be conservative due to the absence of rice plants, whose root exudates can enhance denitrification (18). The combination of MIMS and ^{15}N tracing now provides a powerful approach to directly partition N_2 emissions between soil and fertilizer sources.

Ammonia represents another major pathway of gaseous N loss from paddy fields (19, 20), accounting for approximately 10.5 to 14.8% of applied fertilizer N based on conventional approaches that compare fertilized and unfertilized plots (21). However, these estimates may overlook the contribution of SON mobilized by fertilization. Conventional methods used to quantify gaseous N (NH_3 and N_2) losses, including mass balance calculations and approaches based on fertilizer emission factors (17, 21), typically attribute all measured emissions to applied fertilizer. Yet N fertilization can stimulate SON mineralization and microbial turnover, generating additional soil-derived NH_3 and N_2 that cannot be distinguished from fertilizer-derived losses using these approaches. Consequently, such methods may systematically overestimate fertilizer-derived N_2 and NH_3 emissions.

Similar to N_2 emissions, the respective contributions of fertilizer- and soil-derived NH_3 remain poorly quantified, limiting our understanding of how N fertilization influences the interplay among multiple N loss pathways. This knowledge gap is critical, because NH_3 and N_2 emissions are tightly coupled and can vary across the rice-growing season (9). Early in the season, when rice N uptake is limited, a larger proportion of basal fertilizer N may be lost as NH_3, reducing the substrate available for N_2 emissions, and vice versa, depending on the environmental (e.g., air temperature) and soil conditions (e.g., anaerobic status) (4). Later, as the root system develops, top-dressed N is more efficiently absorbed and both NH_3 and N_2 losses may decline. However, increasing root exudation and radial O_2 release into the rhizosphere can stimulate SOM decomposition and denitrifier activity (22), potentially enhancing soil-derived NH_3 and N_2 emissions (17). To date, no study has systematically quantified NH_3 and N_2 fluxes throughout the rice-growing season while distinguishing soil- and fertilizer-derived sources. This limitation has hindered the development of strategies to simultaneously reduce NH_3 and N_2 emissions from rice paddies.

Rice plants play a critical role in regulating the fate of applied N fertilizer and associated gaseous losses through cultivar-specific differences in N uptake, root O_2 loss (23) and root exudation (24), and soil N transformation rates (25). On the one hand, high-yielding cultivars, such as hybrid rice, generally absorb more fertilizer-derived N, thereby reducing the mineral N pool available for gaseous losses (26). Hybrid rice also releases greater amounts of root-derived dissolved organic carbon (DOC), which can stimulate microbial N immobilization (27), and further decrease the substrate available for NH_3 and N_2 production (10, 24). On the other hand, hybrid rice typically exhibits greater root porosity and radial O_2 loss, which can enhance rhizosphere oxidation, accelerating SON mineralization and nitrification (25), and increase nitrate availability for denitrification. Elevated DOC may also promote the reduction of N_2O to N_2 during denitrification (17). Despite these opposing processes, current evidence suggests that enhanced plant N uptake and microbial immobilization are likely to dominate, resulting in a net reduction in reactive N losses (particularly NH_3 and N_2O) (28), while potentially shifting the sources of gaseous losses such as N_2 from fertilizer N to SON. However, owing to methodological limitations, the mechanisms regulating the dominant N loss pathway in flooded rice systems, particularly N_2 emissions, have rarely been examined in relation to rice cultivars. This knowledge gap limits our understanding of how rice cultivars regulate the complete fate of applied fertilizer N, and constrains efforts to optimize cultivar selection for both high yield and reduced environmental impact.

To address these knowledge gaps, we coupled MIMS and ^{15}N tracing (^{15}N-MIMS; *SI Appendix*, Fig. S1) techniques to a) simultaneously quantify in situ emissions of N_2, NH_3, and N_2O; b) partition their soil- and fertilizer-derived sources; and c) track the complete fate of applied N fertilizer throughout the growing season for two rice cultivars with distinct growth and yield traits: conventional *japonica* rice (CXJ) and hybrid rice (HZY). We hypothesized that a) fertilizer N is the dominant source of all three gaseous N losses, and soil-derived contributions are non-negligible regardless of rice cultivar; b) seasonal tradeoffs exist between N_2 and NH_3 emissions, with NH_3 dominating early-season losses and N_2 dominating in late season; c) conventional methods overestimate N_2 and NH_3 emission factors relative to ^{15}N-MIMS techniques; and d) compared to CXJ, hybrid rice HZY improves fertilizer N use efficiency, stimulates fungal and bacterial N immobilization and reduces N_2, NH_3, and N_2O emissions, thereby enhancing both rice productivity and environmental outcomes.

Results

Different Flux Pattern of Gaseous N Losses. Both rice cultivars (HZY and CXJ) exhibited similar seasonal patterns of gaseous N emissions, but the temporal emissions differed among N species (Fig. 1). NH_3 fluxes peaked shortly after the first basal N application, coinciding with maximum soil NH_4^+-N concentrations (Fig. 1*D*), and reached 7.0 and 8.8 kg N ha^{-1} d^{-1} for HZY and CXJ, respectively (Fig. 1*B*). N_2 fluxes peaked later, following fertilization after the third panicle-initiation, when surface water dissolved oxygen was minimal (Fig. 1*F*), with maxima of 2.5 (HZY) and 1.9 (CXJ) kg N ha^{-1} d^{-1} (Fig. 1*A*). In contrast, N_2O fluxes peaked during mid-season drainage rather than immediately after N fertilization (Fig. 1*C*). Across the rice-growing season, the three fertilization events strongly stimulated NH_3 fluxes and diminished as plants matured. N_2 fluxes, however, showed weaker responses to basal and tillering N fertilization, and their temporal patterns were largely decoupled from changes in soil NH_4^+-N and NO_3^--N contents (Fig. 1 *A*, *E*, and *F*).

N_2 and NH_3 emissions showed a consistent seasonal trade-off across both cultivars (Fig. 2). During the basal fertilization (BF) period, cumulative NH_3 emissions exceeded N_2 emissions by 23% in HZY ($P > 0.05$) and by 45% in CXJ ($P < 0.05$) (Fig. 2*A*). From the tillering stage onward, however, N_2 dominated the gaseous N losses. During the tillering fertilization period (TF), cumulative N_2 emissions were 1.8-fold (HZY, $P < 0.05$) and 1.9-fold (CXJ, $P < 0.05$) higher than NH_3 emissions (Fig. 2*A*). The largest N_2 emissions occurred during the panicle-initiation fertilization period (PF), reaching 24.4 to 30.7 kg N ha^{-1}, compared with 17.9 to 21.2 kg N ha^{-1} in BF and 14.4 to 17.5 kg N ha^{-1} in TF. By contrast, NH_3 emissions during PF were far lower than in BF and TF. As a result, N_2 emissions during PF were 4.9-fold (HZY, $P < 0.01$) and 6.2-fold (CXJ, $P < 0.01$) greater than NH_3 emissions, underscoring a seasonal shift from NH_3-dominated to N_2-dominated gaseous losses (Fig. 2*A*).

Contrasting Dominant Sources of Gaseous N Emissions. The three gaseous N species showed contrasting dominant sources (Fig. 2). The pot experiment showed that seasonal cumulative N_2 emissions ranged from 59.9 kg N ha^{-1} in HZY to 66.1 kg N ha^{-1}

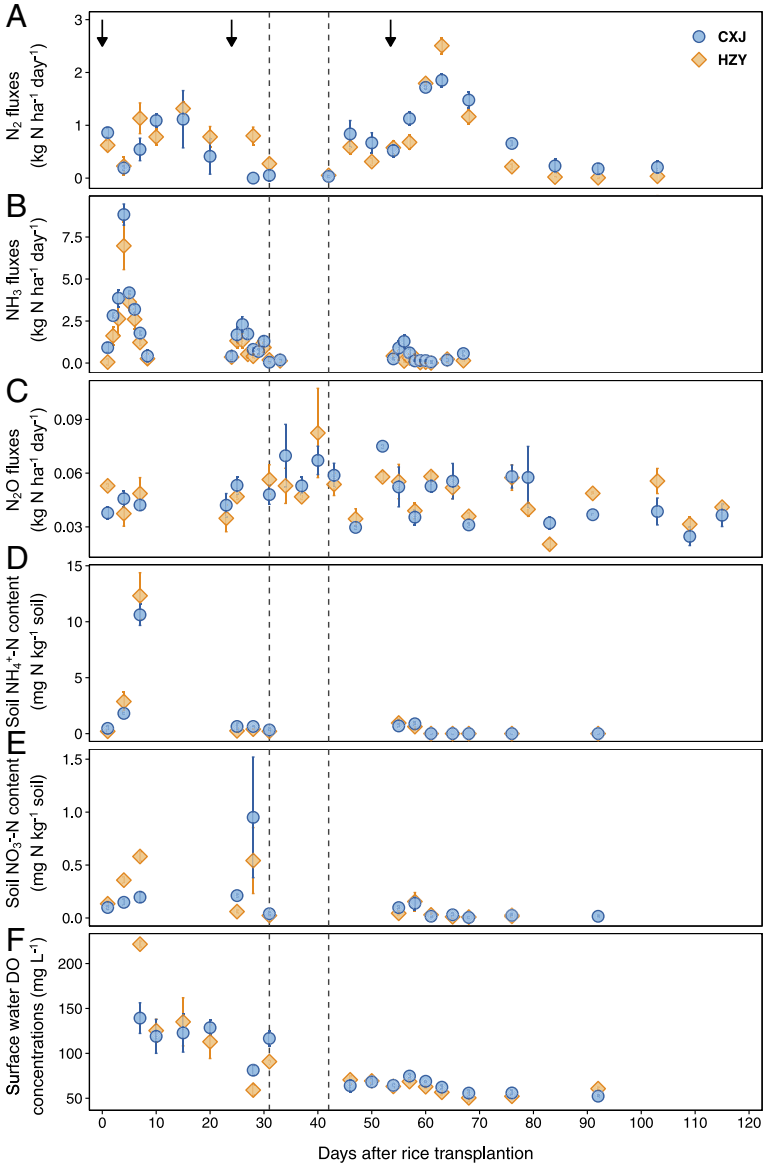

Fig. 1. Seasonal variations in (*A*) N_2, (*B*) NH_3, and (*C*) N_2O fluxes, as well as (*D*) soil NH_4^+, (*E*) NO_3^-, and (*F*) DOC concentrations under different cultivar treatments during the rice-growing season of 2024. CXJ, japonica rice cultivar "Changxiang Jing 1813"; HZY, hybrid rice cultivar "Huazhong You 9326". Error bars indicate SD (n = 3). Arrows indicate nitrogen fertilizer application events. The dashed line indicates midseason drainage period.

in CXJ (Fig. 2*B*), with SON being the primary source for both cultivars. SON dominated N_2 emissions across all growth stages, accounting for 78.3 to 81.4% in BF, 66.2 to 64.9% in TF, and 71.9 to 74.3% in PF (Fig. 2*A*). Field in situ measurements from a 14-y long-term fertilization experiment further confirmed that SON is the major source of N_2 emissions (76.4%) in flooded rice paddies (Fig. 2*D* and *SI Appendix*, Fig. S4). In contrast, NH_3 emissions were mainly fertilizer-derived. Seasonal cumulative NH_3 emissions were 35.9 kg N ha^{-1} in HZY and 40.1 kg N ha^{-1} in CXJ, with fertilizer contributions of 70.8 to 76.5% across the whole season (Fig. 2*A*). N_2O emissions were much smaller (1.37 to 1.42 kg N ha^{-1}) and derived nearly equally from soil (49.6 to 51.5%) and fertilizer (48.6 to 50.4%) (Fig. 2*B*).

Fates of Applied N Fertilizer. Of the 240 kg N ha^{-1} applied, gaseous N losses accounted for 26.6 to 33.1% across the two cultivars, dominated by N_2 (16.0 to 19.4%), followed by NH_3 (10.8 to 13.3%), with N_2O losses being negligible (0.30 to 0.33%) (Fig. 3*A*). Plant uptake represented the largest sink, at 40.2 to 45.0% of applied N. Soil retained 18.7 to 21.2%, of which 3.9 to 5.5% was immobilized in SON pools and 14.8 to 15.7% was assimilated by soil microbes (Fig. 4*A*). Fungi dominated microbial N assimilation (74.9 to 80.4%), whereas bacteria contributed 19.6 to 25.1%.

Effects of Rice Cultivar. The most notable effect of cultivar was a significant reduction in gaseous N loss intensity under hybrid rice (HZY). Compared with *japonica* rice (CXJ), HZY produced 26.9% more biomass and 58.6% higher grain yield (both $P < 0.05$; Fig. 5*A*), leading to a 42.6% decrease in gaseous N loss intensity ($P < 0.05$; Fig. 5*D*). Although absolute reductions in N_2, NH_3, and total gaseous N emissions under HZY (9.3%, 10.2%, and 9.5%, respectively) were not statistically significant ($P > 0.05$; Fig. 2*B*), the greater productivity of HZY translated into markedly lower emissions per unit biomass. Seasonal source partitioning showed that soil-derived contributions to both N_2 and NH_3 were consistently greater in HZY than in CXJ across all growth stages (Fig. 2*A* and *SI Appendix*, Tables S2 and S3). Moreover, HZY was

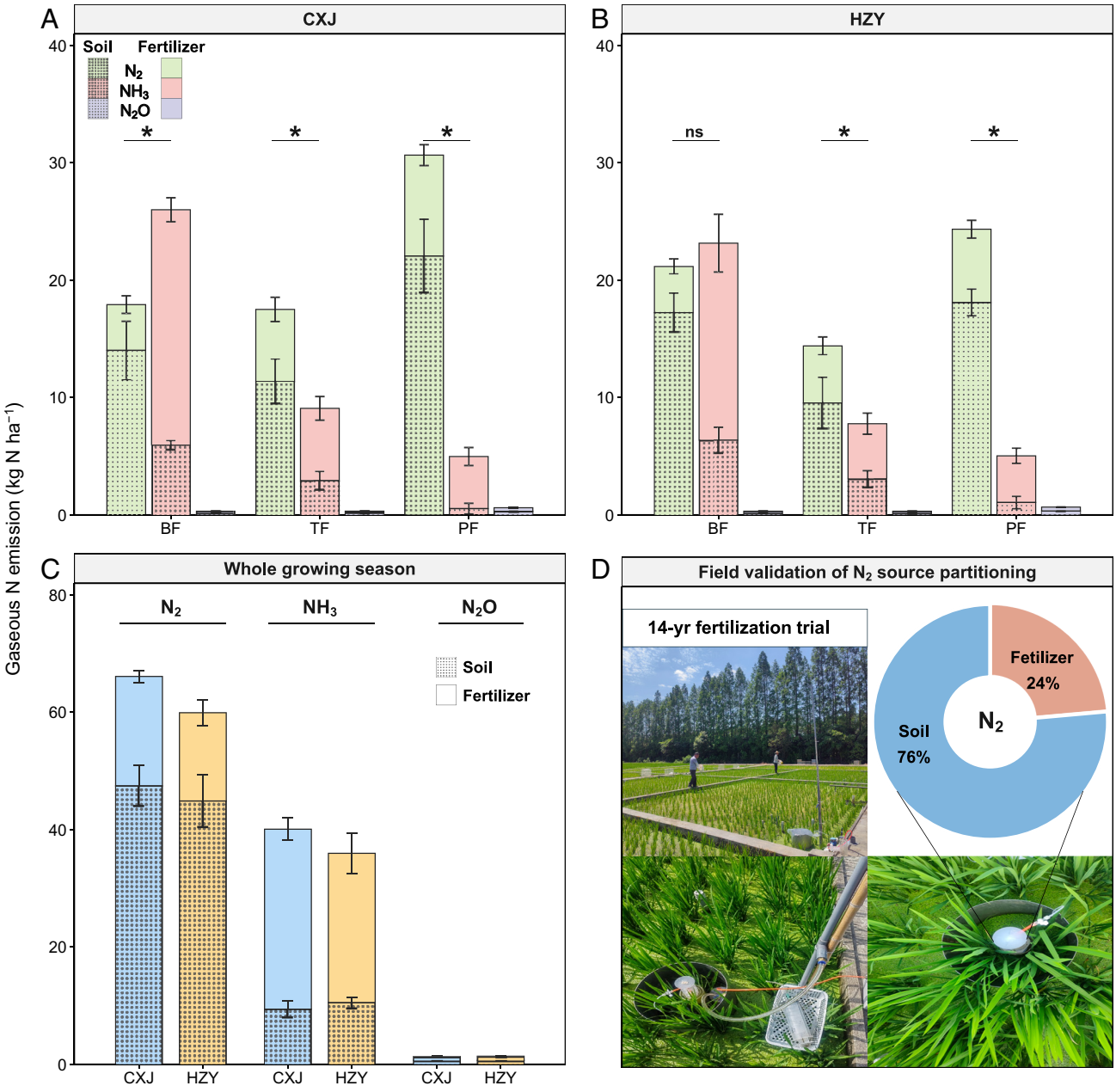

Fig. 2. N_2, NH_3, and N_2O emissions and their respective sources during different fertilization periods from CXJ (*A*) and HZY (*B*) and across the whole rice-growing season (*C*), and field validation of N_2 source partitioning on a 14-y fertilization experiment (*D*). Dark shading denotes soil-derived emissions; light shading denotes fertilizer-derived emissions. BF, TF, and PF denote the basal fertilization, tillering fertilization, and panicle-initiation fertilization periods, respectively. Asterisks (*) indicate significant differences between N_2 and NH_3 emissions at $\alpha = 0.05$. See Fig. 1 for treatment codes.

associated with higher bacterial N assimilation and microbial N use efficiency ($P > 0.05$), despite less N retained in soil or microbial biomass compared with CXJ (Figs. 3*A* and 4 *A* and *B*). Together, these results demonstrate that cultivar choice can substantially improve yield-scaled environmental performance by reducing gaseous N losses per unit of production.

Discussion

Soil, Not Fertilizer, Dominates N_2 Emissions Through a Microbial N Pump. Our results show that soil, rather than fertilizer, is the dominant source of N_2 emissions from flooded paddy fields, regardless of rice-growth stage or cultivar, which is contrary to our first hypothesis (Figs. 2 and 6). This provides direct evidence that SON plays a central role in driving N_2 losses, further supported by the N_2 partitioning field measurements from the long-term fertilization experiment (Fig. 2*D*). These findings challenge the prevailing assumption that fertilizer N is the primary driver of N_2 emissions in flooded rice paddies, and instead reveal a "microbial N pump" mechanism that links fertilizer inputs to soil-derived N losses (Fig. 6). Even under predominantly anaerobic conditions, radial O_2 release from rice roots creates rhizosphere microsites that support coupled SON mineralization, nitrification, and denitrification (29, 30). In these microsites, microbes rapidly assimilate urea-derived NH_4^+ to support growth, creating a C:N stoichiometric imbalance (Fig. 6). To restore this balance, microbes accelerate the decomposition of native SOM, mobilizing SON and releasing additional NH_4^+ that can subsequently be oxidized to nitrate and reduced to N_2 through denitrification (Fig. 6). Although part of the depleted SON pool is replenished through microbial necromass turnover (Fig. 4), this microbial cycling effectively transfers soil-derived N into gaseous losses.

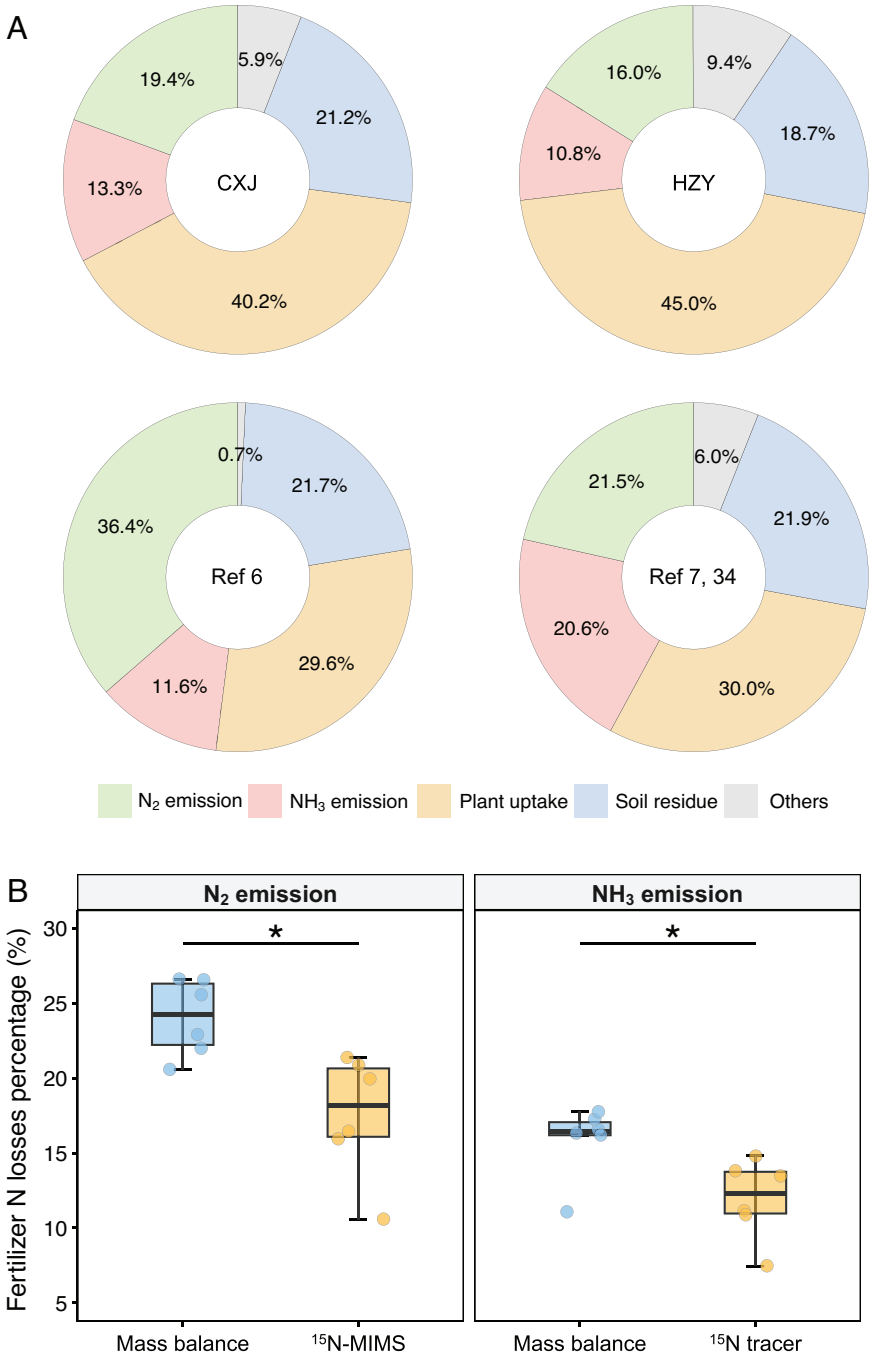

Fig. 3. (*A*) Fate of applied N fertilizer in two rice cultivars in this study compared with previous studies conducted in the same region (refs. 6, 7, and 34); (*B*) percentage of N_2 and NH_3 emissions from fertilizer estimated by conventional approaches versus the ^{15}N tracing method. Asterisks (*) indicate significant differences between mass balance and ^{15}N tracing results at $\alpha = 0.05$. See Fig. 1 for treatment codes.

We conceptualize this coupled process as a microbial N pump (MNP), whereby fertilizer inputs stimulate microbial turnover of SOM and drive the mobilization and loss of soil-derived N as N_2 (Fig. 6), which is supported by the integrated pot and in situ field flux evidence (Fig. 2).

Consistent with the MNP mechanism, a recent isotope-tracing study showed that fertilizer-induced immobilization can increase SON mineralization by 33 to 98.5% (30). Our in situ field measurements further showed that long-term mineral N fertilization increased soil-sourced N_2 emissions by 28.2% (*SI Appendix*, Fig. S4). In addition, urea-derived NH_4^+ can replace interlayer cations in 2:1 clay minerals, weakening cation bridges and accelerating SON decomposition (11, 31). These biological and physicochemical processes increase the supply of soil-derived NH_4^+ to nitrifiers and denitrifiers, thereby amplifying soil-sourced N_2 emissions. The substantially greater microbial assimilation of fertilizer N (32.7 to 35.3 kg N ha^{-1}) compared to SON immobilization (11.4 to 15.5 kg N ha^{-1}) (Fig. 4 and *SI Appendix*, Fig. S5) further highlights the predominance of the MNP mechanism in mediating fertilizer-induced SON mineralization and associated N_2 losses in flooded rice paddies.

Unlike N_2, most NH_3 emissions originated from fertilizer (Fig. 2). These volatilization losses indirectly enhanced soil-sourced N_2 emissions by reducing the pool of urea-derived NH_4^+ available for nitrification–denitrification (16, 17), particularly during BF. At this stage, limited N uptake by young rice roots (32) and high

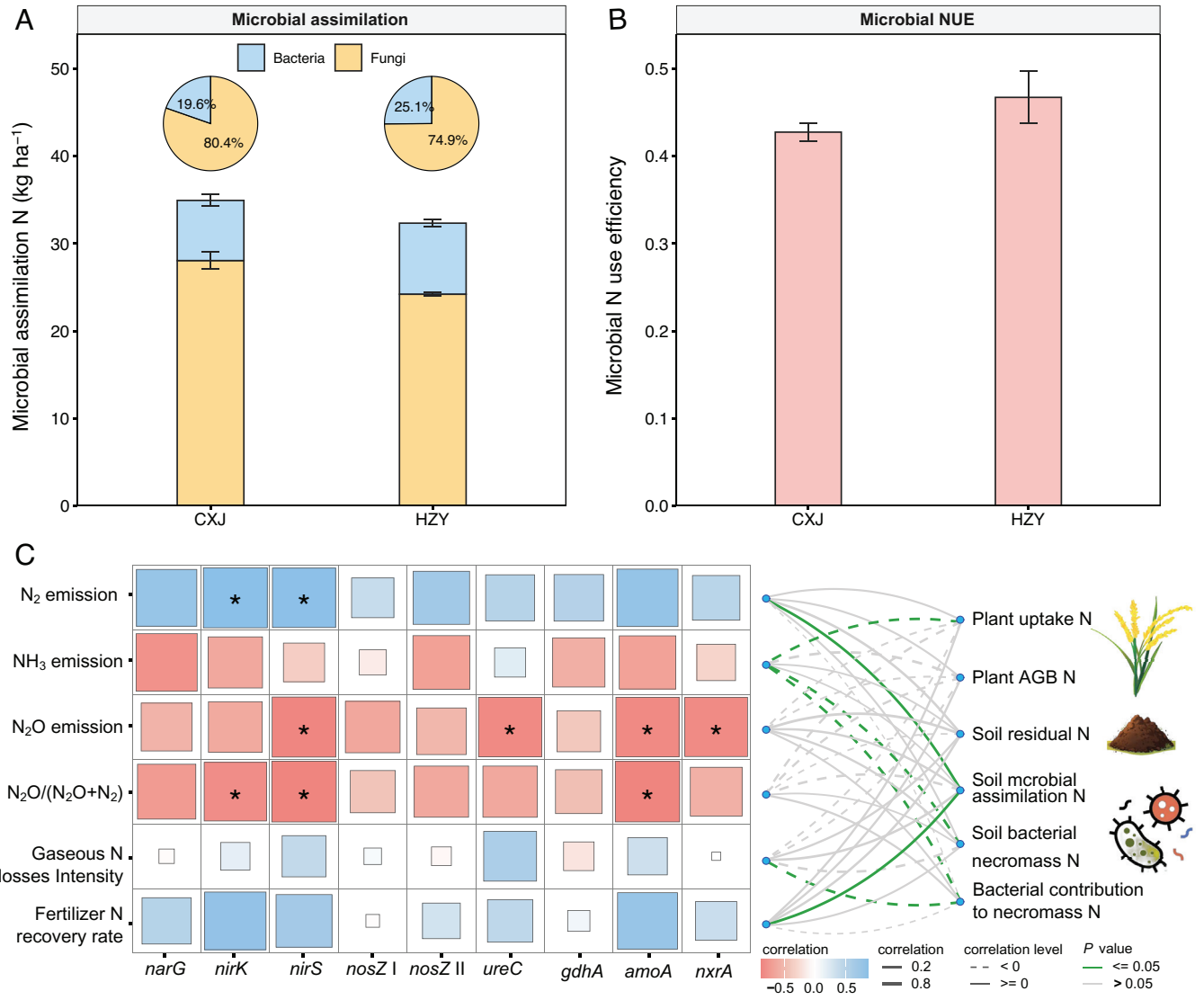

Fig. 4. Microbial assimilation of fertilizer N and the correlation with N turnover. (*A*) Fertilizer-derived N assimilated into bacterial and fungal necromass, and (*B*) microbial N use efficiency in the soils of CXJ and HZY. (*C*) Correlations between microbial N metabolic gene abundance (*narG*, *nirK*, *nirS*, *nosZ* I, *nosZ* II) and gaseous N emissions (N_2, NH_3, N_2O, $N_2O/(N_2O + N_2)$), as well as plant uptake, soil residual N, and microbial assimilated N. Color gradients and square size indicate Spearman's correlation coefficients; asterisks denote significance ($P < 0.05$). Gaseous N emissions were further related to plant uptake, soil residual N, and microbial assimilation N by Pearson's correlation test. Green and gray edges indicate significant ($P < 0.05$) and nonsignificant ($P \geq 0.05$) relationships, respectively. Solid and dashed lines denote positive and negative correlations, with line thickness proportional to Pearson's correlation coefficients.

air temperatures (19) led to substantial NH_3 volatilization (19.1 to 22.8% of applied N), which exceeded plant uptake (18 to 20%) and coincided with peak seasonal fluxes (Fig. 1*B* and *SI Appendix*, Tables S2 and S3). Only 4.1 to 4.5% of applied N was lost as N_2, accounting for 18.6 to 21.7% of total N_2 emissions (Fig. 2*A*). The remaining shortfall was met by SON mineralization, which contributed 78.3 to 81.4% of N_2 emissions during this period, substantially more than during tillering and panicle fertilization. As root systems developed, top-dressed fertilizer was absorbed more efficiently (33), NH_3 losses declined (34), and competition for NH_4^+ between volatilization and nitrification–denitrification lessened (17), increasing the fertilizer contribution to N_2 emissions. Midseason drainage disrupted whole soil anaerobic conditions (35), stimulating microbial N turnover (36, 37) and converting microbial necromass—^{15}N to $^{15}NO_3^-$, which was subsequently denitrified to $^{15}N_2$ upon reflooding. These processes raised the fertilizer share of N_2 emissions to 32.2 to 39.6% during tillering, although SON still dominated (Fig. 2*A*). At panicle fertilization, peak plant N demand and greater C allocation to roots (38), reduced NH_4^+ available for both NH_3 and N_2 losses. Concurrently, rapid root growth and oxygen release intensified rhizosphere priming (39, 40), elevating SON's contribution to N_2 emissions to 71.9 to 74.3% (Fig. 2*A* and *SI Appendix*, Table S2).

Together, these findings reveal a previously underappreciated pathway of fertilization-driven soil N losses in rice systems, mediated by biologically driven N_2 emissions. Although microbial N turnover can partially recycle immobilized N back into soil pools, this process does not fully compensate SON mineralization (Figs. 2*B* and 4*A*). Quantitatively, microbial assimilation of fertilizer-derived N offset 58.7 to 61.6% of soil-derived gaseous N losses, while plant root residue inputs and abiotic stabilization of SON contributed an additional 9.0% and 24.1%, respectively. Even when these pathways are considered together, internal recycling appears insufficient to fully balance soil N fluxes. Sustaining rice productivity while minimizing N losses will therefore require management strategies that maintain soil N stocks and enhance microbial N use efficiency, rather than relying solely on improved fertilizer N recovery.

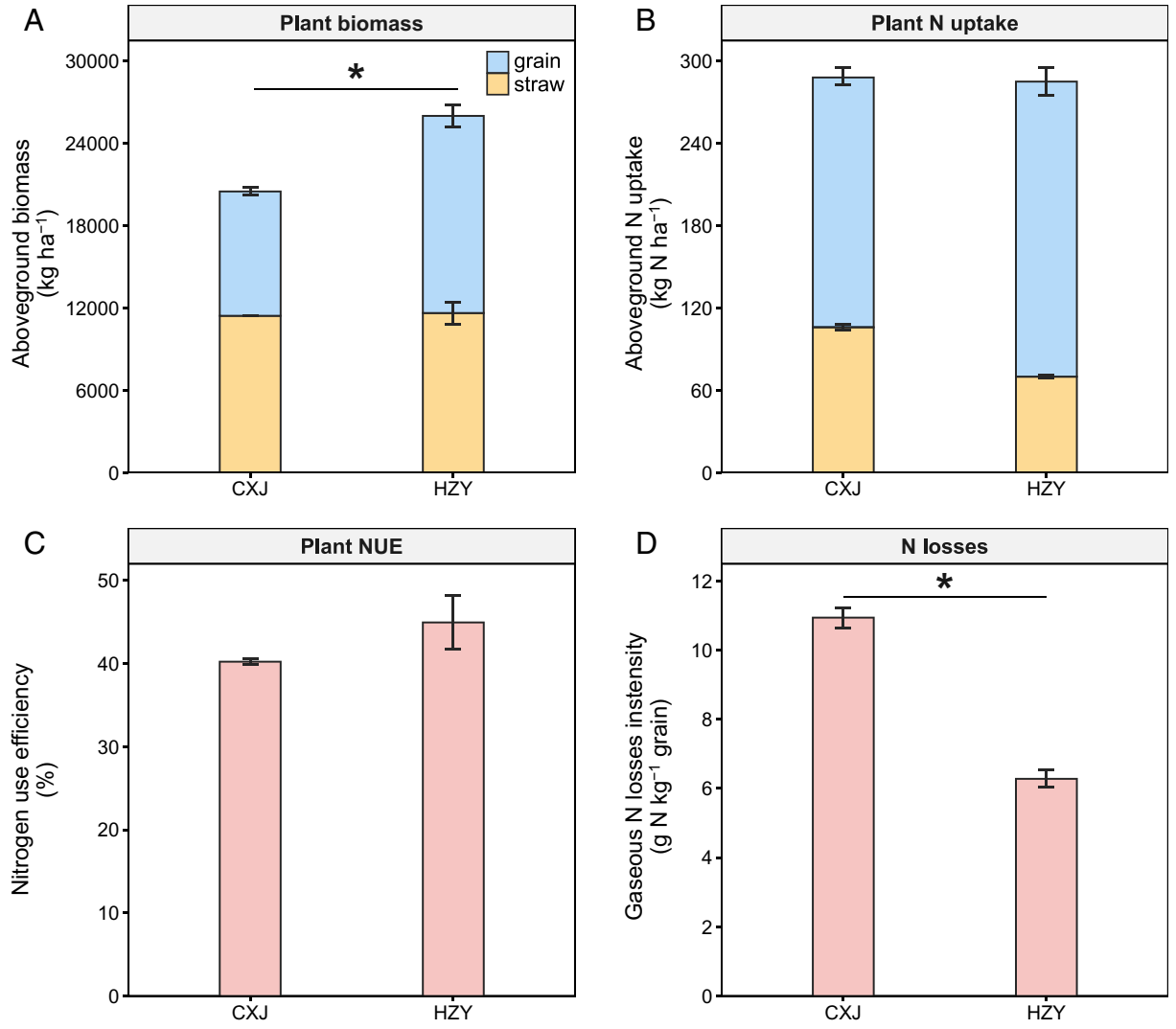

Fig. 5. (*A*) Aboveground biomass, (*B*) N uptake, (*C*) fertilizer N use efficiency, and (*D*) intensity of gaseous N loss under different cultivar treatments during the rice-growing season. Asterisks (*) denote significant differences between cultivars at α = 0.05. See Fig. 1 for treatment codes.

Trade-Offs between NH_3 and N_2 Emissions. Competition among NH_3 volatilization, N_2 production, and plant N uptake for fertilizer- and SON-derived NH_4^+ created a clear seasonal trade-off between NH_3 and N_2 losses, consistent with our second hypothesis (Figs. 2 and 6). Following BF, NH_3 fluxes rose sharply and then declined (0.1 to 2.5 kg N ha^{-1} d^{-1}), whereas N_2 fluxes remained smaller and more stable (0.2 to 1.3 kg N ha^{-1} d^{-1}) (Fig. 1 *A* and *B*). Strong NH_3 losses depleted fertilizer-derived NH_4^+ available for N_2 production (15, 17), while shallow flooding enhanced nitrification (16), as indicated by a two- to 4.5-fold rise in soil NO_3^-. Elevated dissolved oxygen (112 to 222 mg L^{-1}; Fig. 1*F*) further inhibited denitrification (10), reinforcing high NH_3 but low N_2 emissions during this period. During tillering, rice growth cooled the canopy-water-soil microclimate (26, 38), reducing NH_3 volatilization (20). Vigorous plant uptake of fertilizer-derived NH_4^+ suppressed both NH_3 and N_2 losses, but the effect was stronger on NH_3, as plants competed more effectively with volatilization than with soil-sourced N_2 production (11, 17). Consequently, NH_3 declined while N_2 emissions increased. By panicle fertilization, expanded root systems and higher N demand reduced NH_3 losses to negligible levels (4.9 to 5.1 kg N ha^{-1}) (Fig. 2). At the same time, declining dissolved oxygen and abundant root-derived DOC stimulated denitrification (9, 18), producing peak soil-sourced N_2 fluxes. This seasonal pattern of low NH_3 but high N_2 at panicle fertilization completed the trade-off cycle. These dynamics provide mechanistic guidance for the coordinated mitigation of NH_3 and N_2 emissions. For instance, applying a urease inhibitor with basal fertilizer could reduce NH_3 volatilization (4, 41) and associated SON priming, whereas nitrification inhibitors would be more effective when used with topdressing at tillering and panicle fertilization, when strong root NH_4^+ uptake favors suppression of both NH_3 and N_2 losses (16).

Substantial Soil Contributions to N_2 Losses Challenge Conventional Estimates. The substantial contribution of SON to gaseous N losses, particularly N_2, indicates that traditional approaches based on fertilizer emission factor (EF_{Trad}) and mass-balance systematically overestimate fertilizer-derived emissions. Using a ^{15}N-tracer, we quantified NH_3 losses as 10.8 to 13.3% of applied fertilizer N ($EFNH_{3-15N}$), significantly lower than the 15.1 to 16.7% ($EFNH_{3-Trad}$) calculated from the same dataset using conventional methods ($P < 0.05$; Fig. 3*B*). Direct measurements with the ^{15}N–MIMS technique showed that 16.0 to 19.4% of applied N was lost as N_2 (EFN_{2-MIMS}; Fig. 3*A*), compared with 21.6% and 36.4% reported by Zhao et al. (7, 34) and Ju et al. (6) using a traditional ^{15}N mass balance (EFN_{2-Trad}). Even when applied to our dataset, EFN_{2-Trad} (24.1%) remained significantly higher than EFN_{2-MIMS} (17.6%) across rice cultivars ($P < 0.05$;

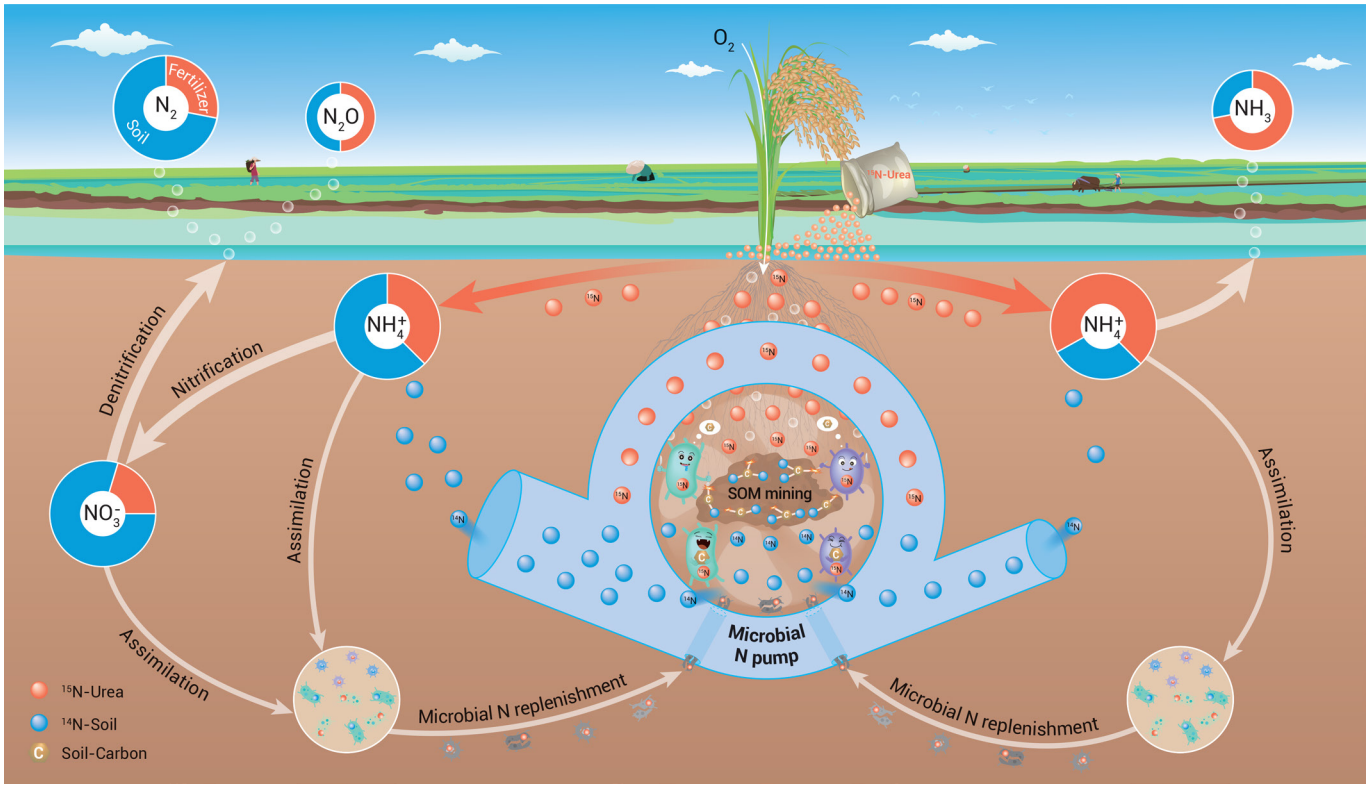

Fig. 6. A microbial nitrogen pump driving distinct sources of soil gaseous nitrogen losses from flooded rice systems. Microbes rapidly assimilate urea-derived NH_4^+ (^{15}N-Urea) to support growth, creating a carbon:nitrogen stoichiometric imbalance. To restore this balance, microbial activities accelerate the decomposition of native SOM, mobilizing soil organic nitrogen (SON) and releasing additional NH_4^+-N (^{14}N-Soil). This N can subsequently be oxidized to nitrate and reduced to N_2 through denitrification, causing SON (SOM), rather than fertilizer, to become the dominant source of N_2 emissions. The mineralized SON is only partially replenished through microbial N turnover. In contrast, NH_3 emissions are largely fertilizer-derived, whereas N_2O originates from soil and fertilizer sources in similar proportions.

Fig. 3*B*), isolating methodological bias. These results support our third hypothesis: Conventional methods overestimate NH_3 and N_2 emissions by neglecting SON contributions.

The ^{15}N–MIMS technique provides more accurate in situ estimates of N_2 losses than first-generation MIMS–soil core incubations, which exclude rice plants (15, 42). MIMS–Soil studies reported 11.9 to 13.5% N_2 loss (16, 17), well below ^{15}N–MIMS values, because they omit plant-mediated processes such as O_2 transport stimulating SOM mineralization and nitrification (25), and root-derived DOC enhancing denitrification (8, 43). Scaling cultivar-averaged emission factors derived from the pot and long-term fertilization experiment ($EFN_{2–MIMS}$, $EFNH_{3–15N}$) to global irrigated paddies yields annual losses of ~2.58 ± 0.6 Tg N as N_2, and 1.76 ± 0.39 Tg N as NH_3 (total 4.34 ± 0.99 Tg N y^{-1}) (*SI Appendix*, Fig. S6). Traditional approaches estimate 5.87 ± 0.73 Tg N y^{-1}, overstating losses by 1.53 ± 0.26 Tg N y^{-1} (~35%), equivalent to ~30% of fertilizer N applied in Chinese paddies. While these numbers provide a first approximation, they should be interpreted cautiously, as climate, soils, cultivars, and management practices can influence emission factors, and regional variability may further affect global estimates. Nonetheless, the comparison highlights clear discrepancies between the ^{15}N–MIMS technique and conventional methods.

These discrepancies have major implications. Flooded rice (~160 Mha) represents a substantial anthropogenic N_2 source, yet this flux is absent from atmospheric inventories. By inflating fertilizer-derived losses and omitting SON contributions, conventional approaches distort N partitioning in agroecosystem models (9, 13, 44), misguide NH_3 abatement strategies (45), and underestimate the scale of reactive N loss (46). The ^{15}N–MIMS technique provides low-bias (14), process-inclusive measurements that can recalibrate emission factors in global databases and improve paddy representation in Earth system models. Revising gaseous N budgets with such measurements is essential to narrow uncertainties in the global N cycle, and target mitigation strategies toward true sources and magnitudes of loss. To further strengthen global extrapolations, multisite and multiyear ^{15}N–MIMS experiments across major rice-producing regions are needed. Such efforts would capture climatic, soil, and management variability, yielding more representative emission factors and robust global N budgets, and providing a stronger foundation for targeted mitigation strategies.

Hybrid Cultivar Benefits Rice Production and Gaseous N Reduction Through Stimulating Plant and Microbial N Use Efficiency. Substantial gaseous N losses from flooded paddy fields (97.3 to 107.5 kg N ha^{-1}) highlight the urgency of developing mitigation strategies that sustain yields while reducing environmental impacts. Consistent with our fourth hypothesis, hybrid rice offers a "win–win" solution, combining high productivity with lower yield-scaled gaseous N losses. Although the absolute reductions in individual gases were not statistically significant, the 42.6% decrease in gaseous N loss intensity ($P < 0.05$) demonstrates a substantial environmental benefit per unit of rice produced.

Two cultivar-dependent mechanisms underpin this effect (*SI Appendix*, Fig. S7). First, HZY captured more applied N in grain and biomass, as indicated by higher fertilizer N use efficiency

(Fig. 5*C*), reducing fertilizer-derived N available for volatilization and denitrification. This is supported by a negative correlation between plant ^{15}N uptake and $^{15}NH_3$ emissions ($P < 0.05$; Fig. 4*C*). Across growth stages, HZY reduced fertilizer-sourced NH_3 by 10.5 to 23.7% and fertilizer-sourced N_2 by up to 27.3% (*SI Appendix*, Table S2). Second, cultivar traits influenced rhizosphere redox and C inputs (25, 39), shifting N source partitioning. During BF, greater root porosity and oxygen release raised floodwater DO (Fig. 1*F*), enhancing SOM mineralization and nitrification (16) and increasing soil-sourced N_2. At tillering and panicle stages, however, higher N uptake drew down both soil and fertilizer pools (*SI Appendix*, Table S3), reducing N_2 emissions despite enhanced DOC exudation and SON mineralization, which is evidenced by much lower denitrification gene abundances *nirK* (–34.4%), *nirS* (–25.4%), and *nosZ* (–41.7%) in HZY (*SI Appendix*, Table S4). These stage-specific effects yielded a net seasonal reduction of 10.2% in N_2 emissions under HZY.

Cultivar effects also extended to microbial N use efficiency (Fig. 4 and *SI Appendix*, Fig. S7). In HZY, abundant root exudates supplied labile C that stimulated microbial communities (47), particularly bacteria capable of efficient NH_4^+ assimilation (48, 49), incorporating mineral N into biomass rather than releasing it as gaseous N (50). This enhanced microbial N use efficiency increased the proportion of assimilated N allocated to biomass production relative to respiratory losses (51, 52). Consequently, even though less fertilizer N remained in soil or microbial pools by season's end, the microbial N pool that persisted was more efficient in turnover and function (53). This efficient microbial loop acted as a short-term buffer, temporarily immobilizing reactive N and suppressing peaks in nitrate availability that could otherwise fuel denitrification and nitrifier–denitrification (54). Consistent with this, $^{15}NH_3$ emissions declined significantly with increasing bacterial ^{15}N assimilation. However, microbial N is not a permanent sink: Necromass-derived ^{15}N can be mineralized and subsequently denitrified (55), as indicated by the positive relationship between microbial N assimilation and N_2 emissions.

Together, these results demonstrate that N management strategies aimed at reducing N losses while maintaining soil N stocks must also enhance microbial retention of residual N and synchronize soil N availability with cultivar-specific uptake capacity. Hybrid cultivars such as HZY combine strong N uptake with microbial stimulation that effectively narrows the window for gaseous losses. Future research should explore whether integrating such cultivars with organic N replenishment, urease and nitrification inhibitors, and tailored fertilizer timing could further improve microbial N use efficiency, align soil N supply with crop demand, and sustain long-term soil fertility. By simultaneously enhancing yield and microbial N use efficiency while reducing NH_3 and N_2 emissions, cultivar-informed strategies offer a scalable pathway toward sustainable intensification of rice agriculture.

Materials and Methods

Study Site and Soil Properties. Soil used for the pot experiment was collected from Jiangning District, Nanjing City, China (31°53′ N, 119°06′ E), located in the Yangtze River region with a subtropical monsoon climate and typical rice-wheat rotation. The mean annual temperature is 15.7 °C, the frost-free period averages 224 d, mean annual precipitation is 1072.9 mm. The soil was a paddy soil developed from loess-derived parent material that has been under long-term cultivation. The basic physicochemical properties of the soil (0 to 20 cm layer) were pH 6.5 (soil-water ratio 1:2.5), total N content of 1.8 g kg^{-1}, organic C 15.9 g kg^{-1}, available phosphorus (P) 42.2 mg kg^{-1}, and available potassium (K) 296.8 mg kg^{-1}.

Experimental Design and Management Practices. We conducted a pot experiment to trace the sources of gaseous N emissions from flooded paddy fields cultivated with two rice cultivars with distinct growth and yield traits: the *japonica* rice Changxiang Jing 1813 (CXJ) and the hybrid rice Huazhong You 9326 (HZY). For each cultivar, two treatments were established with twelve biological replicates (three for gaseous N measurements and nine for destructive sampling): i) control, supplied with urea at natural ^{15}N abundance (0.366 atom%); and ii) ^{15}N-labeled, supplied with 40 atom% ^{15}N-enriched urea-N. In addition, CXJ received a zero-N (N0) treatment to quantify background gaseous N losses during the rice-growing season (*SI Appendix*, Fig. S3). Nitrogen was applied at 240 kg N ha^{-1} as urea, following local practice and split among basal, tillering, and panicle stages at a 4:3:3 ratio. Basal applications of P and K were 76 kg P_2O_5 ha^{-1} and 96 kg K_2O ha^{-1}, respectively.

Pots (20 cm diameter × 25 cm height) were filled with 7 kg of air-dried soil. Rice seedlings were transplanted on July 25 in 2024 at two plants per hill, three hills per pot. Destructive sampling occurred on August 30 (basal stage) and September 28 (tillering stage), with plants grown until harvest on November 30 (129-d growth period). After transplanting and BF, pots were flooded to a depth of 5 cm for 32 d, followed by a 7-d mid-season drainage to suppress unproductive tillering and promote root growth. Pots were arranged in a completely randomized design and were rerandomized weekly to minimize potential positional effects. Irrigation resumed with a 1 to 5 cm water layer maintained until November 23, after which soils were allowed to dry naturally during the week before harvest. Detailed management practices are listed in *SI Appendix*, Table S1.

Additionally, an in situ N_2 measurement was conducted in a 14-y long-term fertilization experiment established in 2012 (30°53′ N, 121°23′ E) within a rice–wheat rotation system in the Yangtze region using a conventional *japonica* cultivar (56). The basic physicochemical properties of the soil (0 to 20 cm layer) were pH 7.6 (soil-water ratio 1:2.5), total N content of 1.4 g kg^{-1}, organic C 13.7 g kg^{-1}. The experiment includes a zero-N control (CK) and a mineral N fertilization treatment (200 kg N ha^{-1} applied in split doses at a ratio of 5:3:2), arranged in a randomized complete block design with three replicate plots (7 m × 8 m) per treatment. Phosphorus and potassium fertilizers were applied at 100 kg P_2O_5 ha^{-1} (basal) and 225 kg K_2O ha^{-1} (44% basal and 56% panicle-stage topdressing), respectively. During the 2025 rice-growing season, microplots (35 cm diameter × 60 cm height) were established within each fertilized plot and received 40 atom% ^{15}N-enriched urea at the same application rate to trace N_2 sources. This field measurement aimed to validate the study's main finding that soil, rather than fertilizer, dominates N_2 emissions in flooded paddy fields, by quantifying the relative contributions of soil- and fertilizer-derived N_2 (Fig. 2*D*). The procedure for measuring N_2 fluxes was the same as that used in the pot experiment and is described in the section "Nitrogen flux measurements." Further details are provided in *SI Appendix*, Fig. S4.

Nitrogen Flux Measurements. For both the pot and long-term fertilization experiments, soil N_2 fluxes and their sources were measured in situ using a denitrification sampling device (Patent No. 201922502696.9 and 201911416804.9) combined with ^{15}N tracing (40 atom%) and MIMS (17) (*SI Appendix*, Fig. S1). The device consists of an injection piston, a PVC cylinder, a stainless-steel cylinder, and a transparent PE bottle. The PVC and stainless-steel cylinders are seamlessly connected, with the PVC positioned on top. The piston is movable and fitted within the PVC cylinder, while the PE bottle encases its exterior, forming a sealed system that eliminates atmospheric N_2 interference and preserves near-natural conditions. Sampling is performed nondestructively by pressing the piston, ensuring structural integrity and optimal sealing. This design enables reliable in situ measurement of soil denitrification rates.

After BF, the device was inserted into the soil with minimal root disturbance, ensuring tight soil–cylinder contact. Before sampling, the piston was withdrawn, and the PVC cylinder was filled with distilled water, gently stirred with a glass rod along the inner wall to homogenize the solution and remove air bubbles. The valve was opened, the piston was reinserted vertically to the 500 mL mark, and the valve was immediately closed to prevent air entry at the piston–water interface. To further prevent bubble formation at high temperature, the piston head and attached polyethylene bottle were filled with the same field water used inside the cylinder.

Water samples were collected 2, 14, 16, and 18 h after sealing to capture diel rice growth dynamics and ensure sufficient ^{15}N–N_2 enrichment for source

partitioning. Sampling times were validated by consistent N_2 enrichment slopes between 2 to 14 h and 2 to 18 h (*SI Appendix*, Fig. S2). At each time point, three replicates (12 mL) were collected. To inhibit microbial activity, 20 μL of 5% $ZnCl_2$ was added to each vial in advance. During sampling, the water volume (V) in the PVC cylinder was recorded, the valve opened, and the piston pressed manually until the outflow exceeded 1.5 × the vial volume (12 mL), allowing overflow from the silicone tubing. The vial cap was then sealed immediately to avoid atmospheric contamination. Samples were stored at 4 °C until analysis.

Dissolved N_2 and Ar concentrations were determined by MIMS following Kana et al. (14) and Li et al. (15). Measured N_2/Ar ratios were converted to N_2 concentrations using the Ar solubility equation of Weiss (57). The detection limit for N_2/Ar changes was 0.03%. Isotopic composition was determined from signal intensities of $^{28}N_2$, $^{29}N_2$, and $^{30}N_2$. The signal intensity of $^{14}N_2$ was calculated as $^{28}N_2$ + ½$^{29}N_2$, and $^{15}N_2$ as $^{30}N_2$ + ½$^{29}N_2$, based on the isotopic distribution pattern of N_2 molecules (*SI Appendix*, Fig. S1*B*). N_2 fluxes (μmol L^{-1} h^{-1}) were estimated from four-point linear regression and volume-corrected. Because denitrification accounts for 77 to 92% of nitrate reduction (58), net N_2 production was attributed primarily to denitrification. Fluxes were measured 18 times during the rice season: weekly under baseline conditions and 2 to 3 times per week after fertilization. Daily N_2 emissions were calculated using the linear difference method, and seasonal cumulative emissions were obtained by summing daily fluxes as described in Xia et al. (17). The ^{15}N–MIMS technique provides improved accuracy for direct in situ quantification of N_2 emissions compared to the first-generation MIMS–soil core incubations (15), which excludes rice plants.

The contribution of fertilizer-derived N to total N_2 emissions was calculated as

$$P_{\text{fertilizer}}N_2 = \frac{E^{15}N_2 + F_N \times (1 - AT_F) \times EF_{\text{fertilizer}}}{E^{14}N_2 + E^{15}N_2}, \quad [1]$$

where $E^{14}N_2$ and $E^{15}N_2$ are the cumulative emissions of $^{14}N_2$ and $^{15}N_2$ fluxes (kg N ha^{-1}), respectively; $EF_{\text{fertilizer}}$ is the N_2 emission factor of fertilizer N; F_N is the N application rate (240 kg N ha^{-1}); and AT_F is the ^{15}N abundance (%) of the applied fertilizer.

The N_2 emission factor of fertilizer N was calculated as

$$EF_{\text{fertilizer}} = \frac{E^{15}N_2}{F_N \times AT_F}. \quad [2]$$

Ammonia volatilization was measured using a modified continuous air-flow enclosure method (11). Chambers were 7 cm in diameter and 24.5 cm in height, with effective volume adjusted according to insertion depth in soil or water. Air was pumped through at 15 to 20 chamber volumes per minute, and volatilized NH_3 was trapped in 100 mL of 0.05 mol L^{-1} H_2SO_4 solution. Gas was sampled for 2 h twice daily, from 08:00 to 10:00 and 15:00 to 17:00. The mean hourly NH_3 fluxes across both samplings were used as the daily average. Measurements were conducted continuously for 1 to 2 wk after fertilization, depending on sorbent color change (26). Ammonium concentration in the adsorbent solution was determined using a flow injection analyzer (Skalar Analytical, NL) coupled with salicylic acid spectrophotometry. Daily NH_3 volatilization rates were used to calculate cumulative fluxes over the growing season. To partition fertilizer-derived NH_3 emissions, a subsample of the sorbent solution was analyzed for the abundance of $^{15}NH_3$ volatilized from each urea application (11). Briefly, the solution was treated with $CuSO_4$, concentrated to a solid at 70 °C, oxidized to ^{15}NO by alkaline sodium hypochlorite, and analyzed for ^{15}N abundance by isotope mass spectrometry (MAT-251, United States) with an analytical precision of ± 0.02 atom%.

The contribution of fertilizer-derived N to NH_3 volatilization was calculated as

$$P_{\text{fertilizer}}NH_3 = \frac{\sum_{i=1}^{t}\left(F_{NH_3-\text{feritilzed},i} \times AT_{NH_3-\text{fertilized},i} - F_{NH_3-\text{blank},i} \times AT_{NH_3-\text{blank},i}\right)}{\sum_{i=1}^{t} F_{NH_3-\text{feritilzed},i}}, \quad [3]$$

where $F_{NH_3-\text{fertilized}}$ and $F_{NH_3-\text{blank}}$ are the daily NH_3 volatilization rates from the fertilized and blank soils (kg N ha^{-1} d^{-1}), respectively; $AT_{NH_3-\text{fertilized}}$ and $AT_{NH_3-\text{blank}}$ are the corresponding ^{15}N abundance (%) of the sorbent solutions collected from the fertilized and blank soils, respectively; and t is the number of sampling time (days).

N_2O flux was measured using the static chamber method combined with gas chromatography (59) (Agilent 8860, United States). For each pot, a transparent cylindrical chamber (20 cm diameter, 100 cm height) was placed over the plants and sealed with water at the base. Four headspace gas samples were collected at 10-min intervals between 09:00 and 11:00 using an automated gas collection device and stored in 20 mL vials. Fluxes were measured twice per week, with higher frequency following fertilizer application, irrigation events, and mid-season drainage and reirrigation. All samples were analyzed within 12 h by gas chromatography. N_2O fluxes were calculated using the linear difference method, and cumulative seasonal emissions were obtained by summing daily fluxes across the rice-growing period (60). The relative contributions of soil and fertilizer to N_2O emissions were estimated using the conventional emission factor approach (*SI Appendix*, Fig. S3), whereby N_2O emissions from unfertilized controls were subtracted from those of fertilized plots and normalized to the amount of N applied (61).

Soil DNA Extraction and QPCR Analysis. DNA was extracted from 0.5 g freeze-dried soils sampled using a FastDNA SPIN Kit for soil (MP Biomedicals, United States) following the manufacturer's instructions. DNA concentration and purity were assessed with a NanoDrop 2,000 spectrophotometer (Thermo Fisher Scientific, United States). The qualified DNA samples were then dispensed into the 384-well plate as the sample source-plate, while the primer and qPCR reagents to another 384-well plate as the assay source-plate. SmartChip Multisample Nanodispenser (Takara Biomedical Technology) was used to transfer reagents from both sample source-plate and assay source-plate into the micropores of SmartChip MyDesign Chip (Takara Biomedical Technology, Japan). qPCR and fluorescence signal detection were performed in SmartChip Real-Time PCR System (WaferGen Biosystems, United States), and amplification and melting curves were automatically generated.

Soil, Amino Sugar, and Plant N Measurements. Soil NH_4^+-N and NO_3^--N were extracted with 2 M KCl and then determined using a flow injection analyzer (Skalar Analytical, NL). Dissolved oxygen and pH in the field water were determined using a ProQuatro handheld water quality meter (Xylem Company, Germany).

Three pots per treatment were randomly selected for destructive sampling at tillering, elongation, and maturity stages. Plants were harvested, separated into roots, stems, leaves, and grains, dried at 75 °C to constant weight, and weighed. Plant samples were ground, and total N content and $\delta^{15}N$ values were measured using an elemental analyzer coupled with isotope ratio mass spectrometry (EA–IRMS, Germany).

Soil amino sugars were extracted from maturity-stage samples following the Zhang and Amelung method (62) and quantified by gas chromatography (Agilent 7890A, United States). Compound-specific ^{15}N abundance analysis of glucosamine (GluN) and muramic acid (MurN) was determined using isotope gas chromatography–mass spectrometry as described by He et al. (63). The microbial assimilation/immobilization rates of fertilizer N were estimated based on the ^{15}N-labeled amino sugars synthesis rates reported by Li et al. (64).

Nitrogen use efficiency (NUE, %) was calculated as

$$\text{NUE} = 100 \times \left(\frac{U_N - U_0}{F_N}\right) \times AT_F, \quad [4]$$

where U_N is the ^{15}N content of plants fertilized with ^{15}N-labeled urea (kg N ha^{-1}), U_0 is the ^{15}N content of plants in the natural abundance unlabeled treatment. F_N is the N application rate (240 kg N ha^{-1}), and AT_F is the ^{15}N abundance (%) of the applied fertilizer.

Microbial N use efficiency (M_{NUE}) was calculated as

$$M_{\text{NUE}} = \frac{MA_N}{MA_N + ML_N}, \quad [5]$$

where MA_N (kg N ha^{-1}) is the amount of fertilizer N assimilated by microbes, the microbial assimilation N, and ML_N (kg N ha^{-1}) is the amount of fertilizer N lost through microbially mediated gaseous emissions (i.e., N_2 and N_2O losses).

The residual N content of fertilizer in the soil (TNF, mg kg^{-1}) was calculated as,

$$\text{TNF} = TN \times \left(\frac{AT_S - AT_C}{AT_F}\right), \quad [6]$$

where TN (mg kg^{-1}) is the total soil N content, AT_S is the ^{15}N abundance (atom%) in the labeled soil sample, and AT_C is the ^{15}N abundance (atom%) in the unlabeled soil sample.

Gaseous N loss intensity (GNLI, g N kg^{-1} grain) was calculated as

$$\mathrm{GNLI} = 1000 \times \left(\frac{\text{gaseous N loss}}{\text{grain yeild}}\right), \quad [7]$$

where gaseous N loss (kg N ha^{-1}) represents the sum of N_2, NH_3, and N_2O losses, and grain yield (kg grain ha^{-1}) refers to the harvested grain yield.

Statistical Analyses. Data were checked for normality using the Shapiro–Wilk test, and for homogeneity of variances using Levene's test. When both assumptions were met, differences in N_2 emission, NH_3 volatilization, N_2O emission, crop yield, plant N uptake, and NUE among treatments were assessed by one-way ANOVA followed by Duncan tests for multiple comparisons, or by an independent t test for pairwise comparisons. Statistical significance was defined at $\alpha = 0.05$. All analyses and figure plotting were conducted using R software (version 4.3.0).

Data, Materials, and Software Availability. Data used in the study are included in the manuscript and/or *SI Appendix*.

ACKNOWLEDGMENTS. This work was financially supported by the Progress of Strategy Priority Research Program of Chinese Academy of Sciences (XDB0630302), the Major Program of State Key Laboratory of Soil and Sustainable Agriculture (SKLSSA2509), Distinguished Young Scholars Fund (SBK2024010366) and Carbon Peaking and Carbon Neutrality Special Fund for Science and Technology from Jiangsu Science and Technology Department (BM2022002), National Natural Science Foundation of China (42477363 and 42407466), the China Postdoctoral Science Foundation (2025T8180698), and Jiangsu Province Young Scientific and Technological Talents Promotion Plan. K.J.v.G. was funded by the National Environmental Research Council (NE/W001691/1). We thank Prof. Peter M. Groffman for his valuable suggestions. We are also grateful to the colleagues of the T-FACE platform for their assistance.

Author affiliations: [a]State Key Laboratory of Soil and Sustainable Agriculture, Changshu National Agro-Ecosystem Observation and Research Station, Institute of Soil Science, Chinese Academy of Sciences, Nanjing 211135, China; [b]University of Chinese Academy of Sciences, Nanjing 211135, China; [c]Department of Geography, Faculty of Environment, Science and Economy, University of Exeter, Exeter EX4 4RJ, United Kingdom; [d]Pioneer Center for Landscape Research in Sustainable Agricultural Futures, Department of Agroecology, Aarhus University, Aarhus 8000, Denmark; [e]Institute for Meteorology and Climate Research, Karlsruhe Institute of Technology, Garmisch-Partenkirchen 82497, Germany; [f]Institute of Biological and Environmental Sciences, University of Aberdeen, Aberdeen AB24 3UU, United Kingdom; [g]School of Agriculture, Food and Ecosystem Sciences, Faculty of Science, The University of Melbourne, Parkville, VIC 3010, Australia; [h]Department of Land, Air, and Water Resources, University of California, Davis, CA 95616; [i]Institute of Crop Science and Resource Conservation, Soil Science and Soil Ecology, University of Bonn, Bonn 53115, Germany; [j]Institute of Bio- and Geosciences, Agrosphere Institute, Forschungszentrum Jülich, Jülich 52428, Germany; [k]Institute of Applied Ecology, Chinese Academy of Sciences, Shenyang 110016, China; and [l]Eco-environmental Protection Research Institute, Shanghai Academy of Agricultural Sciences, Shanghai 201403, China

Author contributions: X.Y. and L.X. designed research; Y. Lei, Z.W., and K.Y. performed research; Y. Lei and Z.W. contributed new reagents/analytic tools; Y. Lei, Z.W., X.Y., and L.X. analyzed data; and Y. Lei, Z.W., K.Y., K.J.v.G., Y. Liu, H.C., K.B.-B., P.S., D.C., S.K.L., W.R.H., W.A., C.T., W.Z., J.Y., H.H., X.Z., S.Z., X.Y., and L.X. wrote the paper.

1. S. Y. Cai *et al.*, Optimal nitrogen rate strategy for sustainable rice production in China. *Nature* **615**, 73–79 (2023).
2. B. J. Gu *et al.*, Cost-effective mitigation of nitrogen pollution from global croplands. *Nature* **613**, 77–84 (2023).
3. X. Zhang *et al.*, Managing nitrogen for sustainable development. *Nature* **528**, 51–59 (2015).
4. L. L. Xia *et al.*, Can knowledge-based N management produce more staple grain with lower greenhouse gas emission and reactive nitrogen pollution? A meta-analysis. *Glob. Chang. Biol.* **23**, 1917–1925 (2016).
5. L. L. Xia, X. Y. Yan, How to feed the world while reducing nitrogen pollution. *Nature* **613**, 33–34 (2023).
6. X. T. Ju *et al.*, Reducing environmental risk by improving N management in intensive Chinese agricultural systems. *Proc. Natl. Acad. Sci. U.S.A.* **106**, 3041–3046 (2009).
7. X. Zhao *et al.*, Nitrogen balance in a highly fertilized rice-wheat double-cropping system in southern China. *Soil Sci. Soc. Am. J.* **76**, 1068–1078 (2012).
8. Z. L. Zhu *et al.*, Processes of nitrogen loss from fertilizers applied to flooded rice fields on a calcareous soil in north-central China. *Fert. Res.* **18**, 101–115 (1988).
9. H. Y. Zhang *et al.*, Modeling denitrification nitrogen losses in China's rice fields based on multiscale field-experiment constraints. *Glob. Chang. Biol.* **30**, e17199 (2024).
10. K. Butterbach-Bahl *et al.*, Nitrous oxide emissions from soils: How well do we understand the processes and their controls? *Philos. Trans. R. Soc. Lond. B, Biol. Sci.* **368**, 20130122 (2013).
11. X. Zhao *et al.*, Use of nitrogen isotope to determine fertilizer- and soil-derived ammonia volatilization in a rice/wheat rotation system. *J. Agric. Food Chem.* **64**, 3017–3024 (2016).
12. P. M. Groffman *et al.*, Methods for measuring denitrification: Diverse approaches to a difficult problem. *Ecol. Appl.* **16**, 2091–2122 (2006).
13. B. J. Gu *et al.*, Integrated reactive nitrogen budgets and future trends in China. *Proc. Natl. Acad. Sci. U.S.A.* **112**, 8792–8797 (2015).
14. T. M. Kana *et al.*, Membrane inlet mass spectrometer for rapid high-precision determination of N_2, O_2, and Ar in environmental water samples. *Anal. Chem.* **66**, 4166–4170 (1994).
15. X. B. Li, L. L. Xia, X. Y. Yan, Application of membrane inlet mass spectrometry to directly quantify denitrification in flooded rice paddy soil. *Biol. Fertil. Soils* **50**, 891–900 (2014).
16. S. W. Wang *et al.*, Different effects of biochar and a nitrification inhibitor application on paddy soil denitrification: A field experiment over two consecutive rice-growing seasons. *Sci. Total Environ.* **593–594**, 347–356 (2017).
17. L. L. Xia *et al.*, Simultaneous quantification of N_2, NH_3 and N_2O emissions from a flooded paddy field under different N fertilization regimes. *Glob. Chang. Biol.* **26**, 2292–2303 (2020).
18. Z. L. Li *et al.*, Variations and controlling factors of soil denitrification rate. *Glob. Chang. Biol.* **28**, 2133–2145 (2022).
19. P. Xu *et al.*, Fertilizer management for global ammonia emission reduction. *Nature* **626**, 792–798 (2024).
20. F. Zhou *et al.*, Re-estimating NH_3 emissions from Chinese cropland by a new nonlinear model. *Environ. Sci. Technol.* **50**, 564–572 (2015).
21. L. L. Xia *et al.*, Trade-offs between soil carbon sequestration and reactive nitrogen losses under straw return in global agroecosystems. *Glob. Chang. Biol.* **24**, 5919–5932 (2018).
22. K. Butterbach-Bahl *et al.*, Impact of gas transport through rice cultivars on methane emission from rice paddy fields. *Plant Cell Environ.* **20**, 1175–1183 (1997).
23. T. D. Colmer, Aerenchyma and an inducible barrier to radial oxygen loss facilitate root aeration in upland, paddy and deep-water rice (*Oryza sativa* L.). *Ann. Bot.* **91**, 301–309 (2003).
24. L. Xu *et al.*, High yields of hybrid rice do not require more nitrogen fertilizer than inbred rice: A meta-analysis. *Food Energy Secur.* **10**, e276 (2021).
25. P. Ghosh, A. K. Kashyap, Effect of rice cultivars on rate of N-mineralization, nitrification and nitrifier population size in an irrigated rice ecosystem. *Appl. Soil Ecol.* **24**, 27–41 (2003).
26. M. Zhao *et al.*, Mitigating gaseous nitrogen emissions intensity from a Chinese rice cropping system through an improved management practice aimed to close the yield gap. *Agric. Ecosyst. Environ.* **203**, 36–45 (2015).
27. X. B. Li *et al.*, Disentangling immobilization of nitrate by fungi and bacteria in soil to plant residue amendment. *Geoderma* **374**, 114450 (2020).
28. G. Chen *et al.*, Do high nitrogen use efficiency rice cultivars reduce nitrogen losses from paddy fields? *Agric. Ecosyst. Environ.* **209**, 26–33 (2015).
29. Y. Kuzyakov, J. K. Friedel, K. Stahr, Review of mechanisms and quantification of priming effects. *Soil Biol. Biochem.* **32**, 1485–1498 (2000).
30. C. Xu *et al.*, Fertilizer N triggers native soil N-derived N_2O emissions by priming gross N mineralization. *Soil Biol. Biochem.* **178**, 108961 (2023).
31. P. Hart *et al.*, Influence of pool substitution on the interpretation of fertilizer experiments with ^{15}N. *J. Soil Sci.* **37**, 389–403 (1986).
32. L. L. Xia, S. W. Wang, X. Y. Yan, Effects of long-term straw incorporation on the net global warming potential and the net economic benefit in a rice-wheat cropping system in China. *Agric. Ecosyst. Environ.* **197**, 118–127 (2014).
33. F. S. Zhang *et al.*, Integrated nutrient management for food security and environmental quality in China. *Adv. Agron.* **116**, 1–40 (2012).
34. X. Zhao, S. Q. Wang, G. X. Xing, Maintaining rice yield and reducing N pollution by substituting winter legume for wheat in a heavily-fertilized rice-based cropping system of southeast China. *Agric. Ecosyst. Environ.* **202**, 79–89 (2015).
35. Z. Y. Shang *et al.*, Can cropland management practices lower net greenhouse emissions without compromising yield? *Glob. Chang. Biol.* **27**, 4657–4670 (2021).
36. J. W. Zou *et al.*, Changes in fertilizer-induced direct N_2O emissions from paddy fields during rice-growing season in China between 1950s and 1990s. *Glob. Chang. Biol.* **15**, 229–242 (2009).
37. M. Zhou *et al.*, Long-term field measurements of annual methane and nitrous oxide emissions from a Chinese subtropical wheat-rice rotation system. *Soil Biol. Biochem.* **115**, 21–34 (2017).
38. S. B. Peng, K. G. Cassman, Upper threshholds of nitrogen uptake rates and associated nitrogen fertilizer efficiencies in irrigated rice. *Agron. J.* **90**, 178–185 (1998).
39. Y. Kuzyakov, E. Blagodatskaya, Microbial hotspots and hot moments in soil: Concept & review. *Soil Biol. Biochem.* **83**, 184–199 (2015).
40. C. Q. Wang, Y. Kuzyakov, Energy use efficiency of soil microorganisms: Driven by carbon recycling and reduction. *Glob. Chang. Biol.* **29**, 6170–6187 (2023).
41. S. W. Liu *et al.*, A meta-analysis of fertilizer-induced soil NO and combined with NO+N_2O emissions. *Glob. Chang. Biol.* **23**, 2520–2532 (2017).
42. L. L. Xia *et al.*, Greenhouse gas emissions and reactive nitrogen releases during the life-cycles of staple food production in China and their mitigation potential. *Sci. Total Environ.* **556**, 116–125 (2016).
43. J. Wang *et al.*, Patterns and determinants of nitrification and denitrification potentials across 24 rice paddy soils in subtropical China. *Agric. Ecosyst. Environ.* **361**, 108799 (2024).
44. B. B. Pan *et al.*, A global synthesis of soil denitrification: Driving factors and mitigation strategies. *Agric. Ecosyst. Environ.* **327**, 107850 (2022).
45. B. J. Gu *et al.*, Abating ammonia is more cost-effective than nitrogen oxides for mitigating $PM_{2.5}$ air pollution. *Science* **374**, 758–762 (2021).
46. B. Grosz *et al.*, Modeling denitrification: Can we report what we don't know? *AGU. Adv.* **4**, e2023AV000990 (2023).
47. X. F. Huang *et al.*, Rhizosphere interactions: Root exudates, microbes, and microbial communities. *Botany* **92**, 267–275 (2014).

48. Z. N. Chi *et al.*, Effects of nitrogen application on ammonium assimilation and microenvironment in the rhizosphere of drip-irrigated sunflower under plastic mulch. *Front. Microbiol.* **15**, 1390331 (2024).
49. M. Rumeau *et al.*, Root exudate stoichiometry is a key driver of soil N cycling: Implications for forest responses to global change. *Soil Biol. Biochem.* **208**, 109856 (2025).
50. E. Inselsbacher *et al.*, Short-term competition between crop plants and soil microbes for inorganic n fertilizer. *Soil Biol. Biochem.* **42**, 360–372 (2010).
51. M. Mooshammer *et al.*, Adjustment of microbial nitrogen use efficiency to carbon: Itrogen imbalances regulates soil nitrogen cycling. *Nat. Commun.* **5**, 3694 (2014).
52. M. Farrell *et al.*, Soil microbial organic nitrogen uptake is regulated by carbon availability. *Soil Biol. Biochem.* **77**, 261–267 (2014).
53. S. K. Schmidt *et al.*, Biogeochemical consequences of rapid microbial turnover and seasonal succession in soil. *Ecology* **88**, 1379–1385 (2007).
54. D. Huygens *et al.*, Soil nitrogen conservation mechanisms in a pristine south Chilean Nothofagus forest ecosystem. *Soil Biol. Biochem.* **39**, 2448–2458 (2007).
55. I. C. Meier, A. C. Finzi, R. P. Phillips, Root exudates increase N availability by stimulating microbial turnover of fast-cycling N pools. *Soil Biol. Biochem.* **106**, 119–128 (2017).
56. X. X. Zhang *et al.*, Optimizing fertilizer management mitigated net greenhouse gas emissions in a paddy rice-upland wheat rotation system: A ten-year in situ observation of the Yangtze River Delta, China. *Agric. Ecosyst. Environ.* **356**, 108640 (2023).
57. Y. B. Wang *et al.*, Application of water footprint combined with a unified virtual crop pattern to evaluate crop water productivity in grain production in China. *Sci. Total Environ.* **497–498**, 1–9 (2014).
58. J. Shan *et al.*, Dissimilatory nitrate reduction processes in typical Chinese paddy soils: Rates, relative contributions, and influencing factors. *Environ. Sci. Technol.* **50**, 9972–9980 (2016).
59. L. L. Xia *et al.*, Integrating agronomic practices to reduce greenhouse gas emissions while increasing the economic return in a rice-based cropping system. *Agric. Ecosyst. Environ.* **231**, 24–33 (2016).
60. L. L. Xia *et al.*, Greenhouse gas emissions and reactive nitrogen releases from rice production with simultaneous incorporation of wheat straw and nitrogen fertilizer. *Biogeosciences* **13**, 4569–4579 (2016).
61. I. Shcherbak, N. M. Andamp, V. Robertson, Global meta-analysis of the nonlinear response of soil nitrous oxide (N_2O) emissions to fertilizer nitrogen. *Proc. Natl. Acad. Sci. U.S.A.* **111**, 9199–9204 (2014).
62. X. D. Zhang, W. Amelung, Gas chromatographic determination of muramic acid, glucosamine, mannosamine, and galactosamine in soils. *Soil Biol. Biochem.* **28**, 1201–1206 (1996).
63. H. B. He, H. T. Xie, X. D. Zhang, A novel GC/MS technique to assess ^{15}N and ^{13}C incorporation into soil amino sugars. *Soil Biol. Biochem.* **38**, 1083–1091 (2006).
64. X. B. Li *et al.*, Distinct responses of soil fungal and bacterial nitrate immobilization to land conversion from forest to agriculture. *Soil Biol. Biochem.* **134**, 81–89 (2019).